Real-time detection of loosening torque in bolted joints using piezoresistive pressure sensitive layer based on multi-walled carbon nanotubes-epoxy nanocomposites

Abdulkadir Sanli[1,3*], Bilgehan Demirkale[2] and Olfa Kanoun[1]

[1]Chair for Electrical Measurements and Sensor Technology, Technische Universität Chemnitz, Reichenhainer Str. 70, 09126 Chemnitz, Germany

[2]Chair for Assembly and Handling Technology, Technische Universität Chemnitz, Reichenhainer Str. 70, 09126 Chemnitz, Germany

[3]Department of Bioengineering, Royal School of Mines, Imperial College London, SW7 2AZ, London, UK

*Corresponding author: a.sanli@imperial.ac.uk

Abstract—Bolted connections are extensively used in construction and machine design, playing critical roles in various industrial applications. Bolts and screws are, however, prone to loosening or separating due to factors such as shock, vibration, and temperature fluctuations. This self-loosening phenomenon poses a significant challenge to the reliability of bolted connections, necessitating regular inspections to ensure their safety. In this study, we report a cost-effective technique for monitoring bolted joint loosening torque: BoltWISE (**Bolt** loosening detection **w**ith **i**nnovative **se**nsors). BoltWISE employs an innovative sensor element consisting of a piezoresistive, pressure-sensitive layer made from multi-walled carbon nanotube/epoxy nanocomposites coated onto an FR4 substrate, functioning as a washer. This approach provides high sensitivity, durability, linearity, and fast response times, with minimal hysteresis during both the tightening and loosening processes. Finite-element method simulations were conducted to determine the optimal sensor positions, ensuring fast response during bolt tightening and loosening. Our findings highlight BoltWISE as a promising, low-cost solution for efficiently detecting bolt loosening in industrial environments. Its ease of implementation and fabrication make it a valuable tool for improving safety and maintenance practices across various industries.

Keywords—bolt-loosening; smart washer; multi-walled carbon nanotubes; pressure sensing; epoxy resin; piezoresistivity; structural health monitoring

1. Introduction

Bolted joints are crucial for the safe operation of various types of equipment, and they are widely used in many mechanical and civil applications, including manufacturing, power generation, transportation and mining [1]. They are easy to install and disassemble for maintenance, are cost-effective, and can bear relatively heavy loads [2]. These joints, however, tend to loosen over long periods, which can occur separately or in combinations of many factors. For instance, vibration can eventually cause the bolt to "unwind" from the mating threads and the joint to lose its clamp force. In addition, under environmental changes or cyclic industrial processes, loosening of the bolt can also occur due to differential thermal expansion of the material between the bolt and the joint. A sudden force applied to the bolt or the joint due to dynamic loads can cause a mechanical shock, loosening the bolts. If the bolt is not re-tightened in time, this loosening may lead to significant damage to equipment or even catastrophic accidents and disasters [3–5]. Hence, real-time monitoring of the state of bolted joints to prevent them from loosening is highly required.

To date, various techniques have been developed in mechanical and civil structures, as well as in medical dental implants, to observe the state of the bolt, namely whether the joint has been tightened to its full torque [6]. In civil structures, human visual inspection or torque wrench technique using torque meters has often been used for detecting bolt loosening. Here, educated bridge inspectors are appointed to detect and record various bridge structural defects, including bolt loosening. Despite its simplicity and cost-effectiveness, inspection results give many errors due to inconsistency in inspection skills

and the limited abilities of the inspectors to identify the deficiency in bolts, and these approaches cannot monitor the state of the structures online [7]. Other methods for assessing bolt/nut assembly tightness include wave energy dissipation-based linear acoustic approaches [8,9], contact acoustic nonlinearity-based vibroacoustic modulation [9,10], and Hilbert Huang Transform (HHT) method-based detection [11,12]. These techniques often involve costly, frequent audits and labour-intensive processes. Additionally, ongoing research focuses on advanced bolt-loosening detection technologies that employ sensors and transducers, including piezoceramic-based transducers[13–15]. In this approach, a washer acts as a transducer by securing the piezoceramic patch between two pre-machined flat metal rings. This setup requires, however, additional costly components for the data acquisition. Conventional metallic strain gauges are used as washers or integrated bolts [16,17]. Even though this approach yields quite good accuracy, it is expensive and, therefore, can be applied only for experimental applications. Deep learning-based bolt loosening detection systems[18–20], while at the forefront of innovation, face limitations due to their reliance on labelled training data, which may not capture the full spectrum of real-world variations and conditions. *In-situ* inspection methods, including visual inspection, such as image processing methods and smart monitoring techniques, i.e., acoustic, elastic wave, electromechanical impedance, magnet field, and RFID sensor tag, etc. [21–26] have been studied. Sun et al. [27] proposed bolt-loosening detection for steel bridge bolt joints via image processing. This method captures images of bolt joints and calculates rotation angle changes with a specialized algorithm. Despite offering quantitative results and scalability to larger structures, detecting bolt changes is challenging due to minor bolt length variations. Sun et al. [25] utilized Lamb wave phased array theory in the unmanned aerial vehicle wing

box to identify the screw loosening in the structure. This method controls the beam steering by controlling the time delay of the signals to scan the structure. These proposed approaches, however, require complex and costly monitoring systems or complicated algorithms.

In this work, we report our real-time bolt loosening monitoring platform: BoltWISE (**Bolt** loosening detection **w**ith **i**nnovative **s**ensors), a simple and cost-effective technique for monitoring loosening torque on bolted joints. Unlike many existing methods that require complex and expensive instrumentation, BoltWISE offers a practical solution that can be scaled to various industrial applications. The system comprises a washer coated with a pressure-sensitive piezoresistive MWCNTs/epoxy nanocomposite layer (**Fig. 1**). Here, we deposited a pressure-sensitive layer on a glassy-epoxy FR4 substrate by a stencil printing technique, which is then located between the screw washer and nut. We have extensively characterized the pressure-sensitive sensor layer by investigating the dispersion state of the nanocomposite and developed a finite element model (FEM) to define the most appropriate location of the sensor by monitoring the amount of stress and stress distribution on the substrate and the sensor layer. Last, we studied the piezoresistive response of the sensor under different tightening and loosening torques to determine its sensitivity, stability, response time and linearity. BoltWISE provides a streamlined, scalable, and efficient solution that is expected to reduce maintenance costs and prevent potential structural failures in critical industries such as aerospace, automotive, and civil infrastructure.

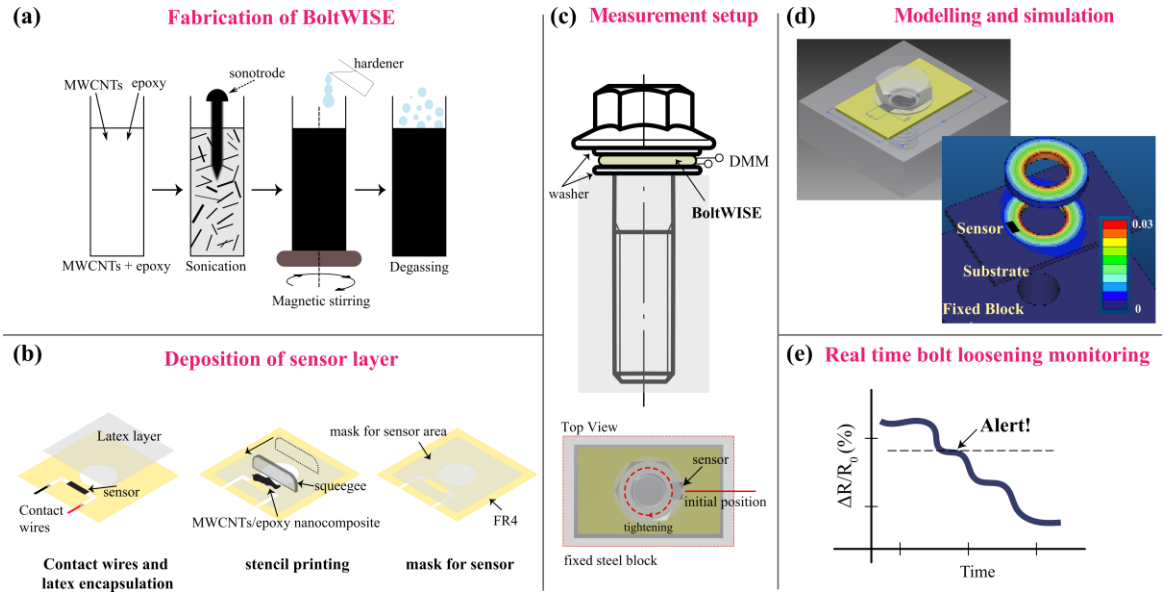

Figure 1: Fabrication and working principle of BoltWISE. (a) Schematic representation of the synthesis and (b) deposition of MWCNTs/epoxy nanocomposite layer on FR4 substrate. (c) Integration of the BoltWISE between two washers and top view of the measurement setup showing the location of the sensor. (d) Modelling and FEM simulation of the BoltWISE tightened in a fixed steel block under the load to define the most suitable location for the sensor. (e) Real-time bolt torque loosening monitoring based on the relative resistance change; illustrations not to scale.

2. Results and discussion

Nanocomposite synthesis: The as-received MWCNTs from Southwest Nano Technology have a 95 % purity, an outer diameter of 6 - 9 nm and a length of < 1 µm. A concentration of 1 wt.% MWCNTs is directly mixed with epoxy resin L20 (Bisphenol A-epichlorohydrin), and then the mixture is sonicated using a horn sonicator (Bandelin GM3200) for 30 min at 30 W power (**Fig. 1a**). The composite mixture is then mixed with a magnetic stirrer at 400 rpm for 2 h. Next, hardener (EPH-161), at a 1:10 ratio is added to the MWCNTs/epoxy mixture, and the solution is further mixed using a magnetic stirrer at

400 rpm for 10 minutes. The final mixture is put into a vacuum chamber to allow degassing that occurs during mixing processes.

Sensor Characterization: The homogeneous distribution (dispersion) of MWCNTs within the epoxy matrix, as observed in the SEM image is crucial for ensuring a repeatable and sensitive sensor response[28,29]. Despite the presence of some partial agglomerations, the MWCNTs are found to be randomly and uniformly distributed (**Fig. 2a**). Furthermore, AFM topography (**Fig. 2b**) reveals a relatively smooth surface, with MWCNTs not visibly present on the surface, suggesting their burial within the matrix. Nevertheless, the quasi-homogeneous distribution of the MWCNTs network within the epoxy polymer matrix, confirmed by the AFM image, underscores the importance of achieving uniform dispersion for optimal sensor performance.

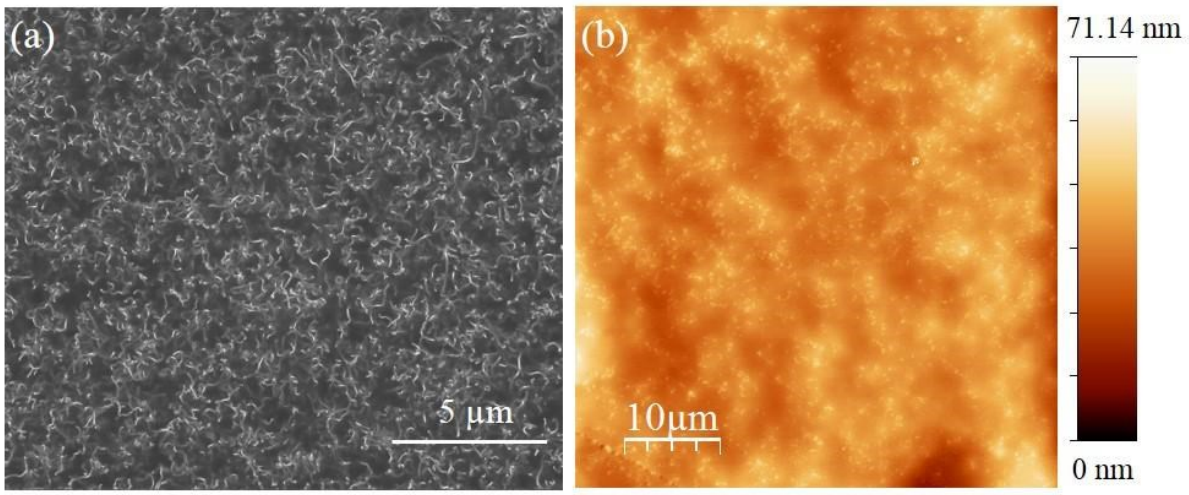

Figure 2: Surface morphology of the (MWCNTs)/epoxy-based pressure-sensitive nanocomposite with a 1 wt.% MWCNTs concentration. In (**a**), scanning electron microscopy (SEM) was utilized to examine the surface structure, while in (**b**), atomic force microscopy (AFM) was employed for topographical analysis. Notably, the AFM image's dimensions are 50 µm by 50 µm, with a scale of 10 µm. The AFM image acquisition rate was set at one-line s^{-1}. The analysis was conducted utilizing commercial WSxM SPM software.

Finite element modelling: Computational modeling and simulation of the nanocomposite measurement system play a significant role in its development. Hence, we built a 2-D FEM

model to ensure the safety of the measurement system, to understand the stress and displacement over the sensor area, as well as to determine the ideal sensor position during tightening. It is important to note that the forces generated by the tightening of the bolt cannot be defined with a single (ordinary, standard) force definition because they are structurally formed between the bolt and the toothed steel block (**Fig. S2**).

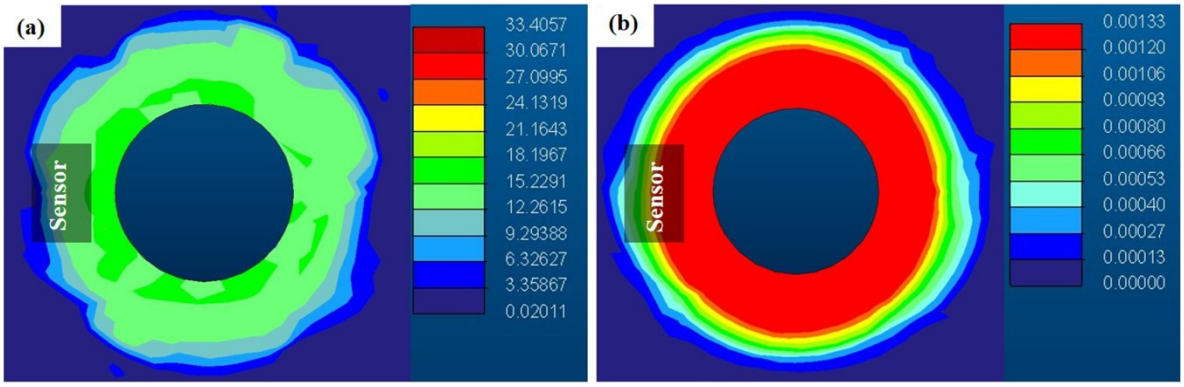

Figure 3: 2-D FEM model of the bolt when the screw is tightened up to 10 Nm of torque. (**a**) The stress (in MPa) distribution across the bolt structure is depicted. The color gradient represents varying stress magnitudes, with warmer colors indicating higher stress levels and cooler colors indicating lower stress levels. The position of sensors within the bolt structure is marked, allowing for precise monitoring and analysis of stress variations at specific points along the bolt's length. (**b**) The displacement distribution (in mm) of the substrate material under the applied tightening torque. Similar to the stress distribution visualization, the color gradient illustrates varying displacement magnitudes, with warmer colors representing larger displacements and cooler colors indicating minimal displacement.

We observed that the amount of stress is more dominant around the bolt, gradually decreasing as it gets away from the sensor area. Furthermore, it is calculated that under 10 Nm of torque, up to 21 MPa of stress corresponding to ~31.5 kN is being applied to the sensor (**Fig. 3a**). The substrate displacement from the bolt and sensor area is also calculated in **Fig. 3b**. As expected, the maximum displacement occurs around the inner area of the bolt when tightened and decreases towards the outer. Under the maximum torque of 10 Nm, the displacement on the sensor area is calculated to be in the range of 0.9 to 1.3 μm, which

again confirms that the sensor was in the optimal position for monitoring the bolt loosening.

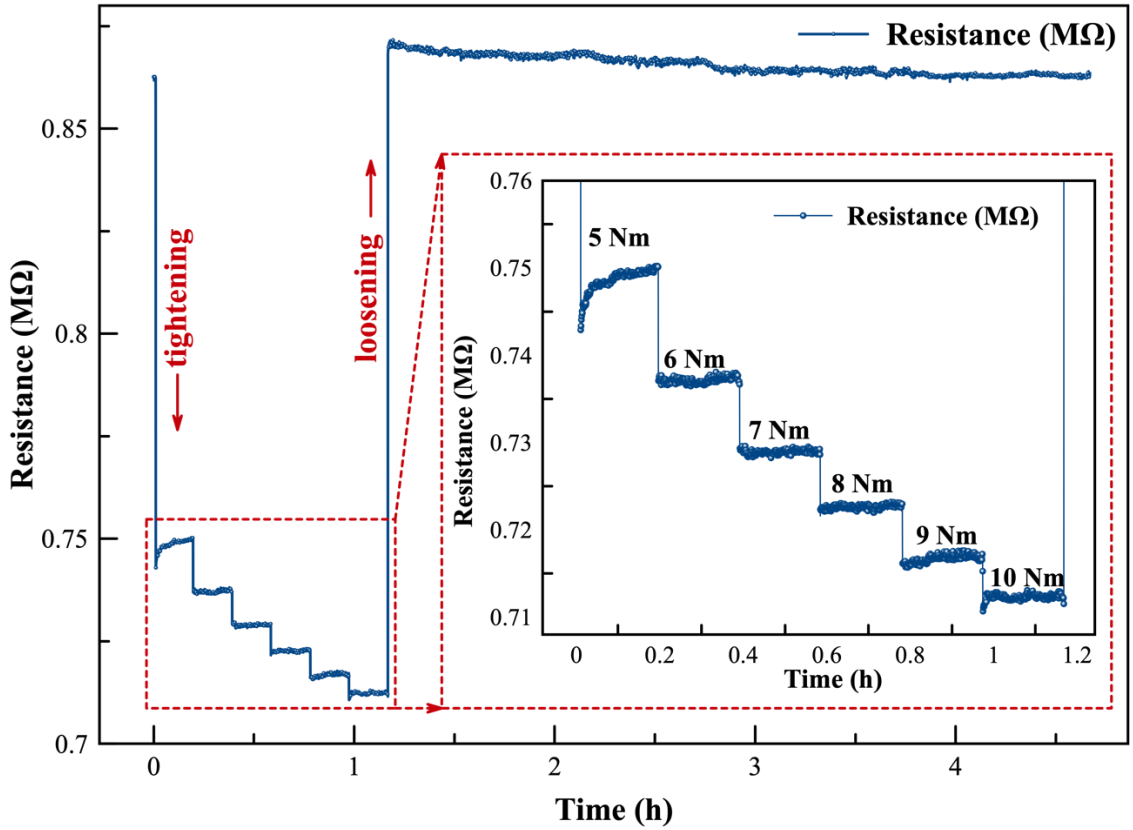

Figure 4: The resistance profile of the sensor after tightening and loosening the bolt. The inset figure displays the piezoresistive response of the sensor at various torque levels, ranging from 5 Nm to 10 Nm, incrementing by 1 Nm torque. Throughout this experiment, measurements were taken continuously for 30 minutes at each torque step.

Piezoresistive response of the pressure-sensitive nanocomposite layer: **Fig. 4** shows the resistance change of the MWCNTs/epoxy nanocomposites under tightening/loosening of the screw. We observed that the resistance of the sensor decreases with the tightening and increases with the loosening of the screw, with a quite sensitive response. With the application of the initial first 5 Nm torque, the sensor resistance decreases from 0.86 MΩ to

0.75 MΩ (around 12.8 %), and it increases up to 0.71 MΩ under 10 Nm of the tightening torque.

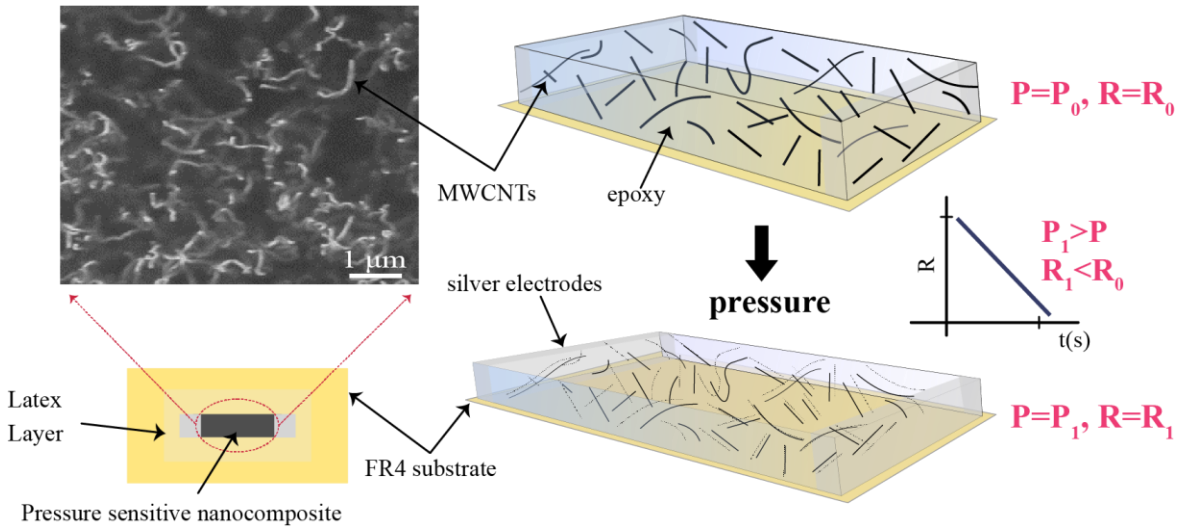

Figure 5: A schematic illustration of the piezoresistivity mechanism observed in MWCNTs/epoxy nanocomposites under applied force, accompanied by a corresponding SEM image showcasing the uniform dispersion of MWCNTs network within the epoxy resin polymer matrix. As pressure is exerted, the interconnected network of MWCNTs within the composite material responds dynamically by drawing closer to each other. This spatial rearrangement of the MWCNTs network leads to a notable reduction in electrical resistance across the applied pressure.

The inset image (**Fig. 4**) shows that the sensor is also quite sensitive under the 1 Nm of tightening/loosening torque. Both experimental and numerical studies have demonstrated that the piezoresistivity mechanism in the MWCNTs/polymer nanocomposites under pressure can be attributed to three main factors: (i) changes in tunnelling resistance within the CNTs network, (ii) breakage or loss of contacts between the CNTs in the polymer matrix, (iii) piezoresistivity of individual CNTs themselves[30–32].

In the case of the CNTs/polymer-based nanocomposites, CNTs are separated from each other by a small distance due to the inevitable gap between CNTs arising from the polymer host. Hence, the tunnelling effect dominates the nanocomposite's conduction mechanism under load [33,34]. The tunnelling resistance is $R_{tunnel} \propto (d)\ exp\ (cd)$, where c is

constant, and *d* is the distance between CNTs [35,36] Considering the aforementioned effect, the decrease in the resistance of the MWCNTs/epoxy nanocomposite under pressure can be explained as follows (**Fig. 5**). As confirmed through SEM/AFM images, MWCNTs are randomly and homogeneously distributed within the epoxy polymer matrix, which gives a specific resistance value. Under the applied pressure, MWCNTs get closer to each other, reducing the distance between them and resulting in a certain decrease in the total resistance, which strongly depends on the MWCNTs concentration.[37]

Besides the high sensitivity of the sensor under-tightening and loosening, the hysteresis and response time of the sensor are also important aspects to investigate. Hysteresis in the nanocomposites occurs due to the viscoelastic nature of the polymer as well as the interaction between the fillers and polymers [38]. Depending on the strength of the interfacial binding between nanomaterial and polymers, CNTs/polymer-based nanocomposites give different hysteresis behaviours under load. While strong interfacial binding results in a lower hysteresis, weak interfacial binding results in a high hysteresis due to the high possibility of the slippage and irreversible rearrangement of CNTs [22,39]. The initial resistance of the sensor is 0.862 MΩ ± 0.04 %, and it changes to 0.865 MΩ ± 0.04 % after the tightening and loosening of the screw, which corresponds to a negligible relative resistance change of 0.3 % that is attributed to the strong interfacial binding between MWCNTs and epoxy polymer matrix (**Fig. 6**).

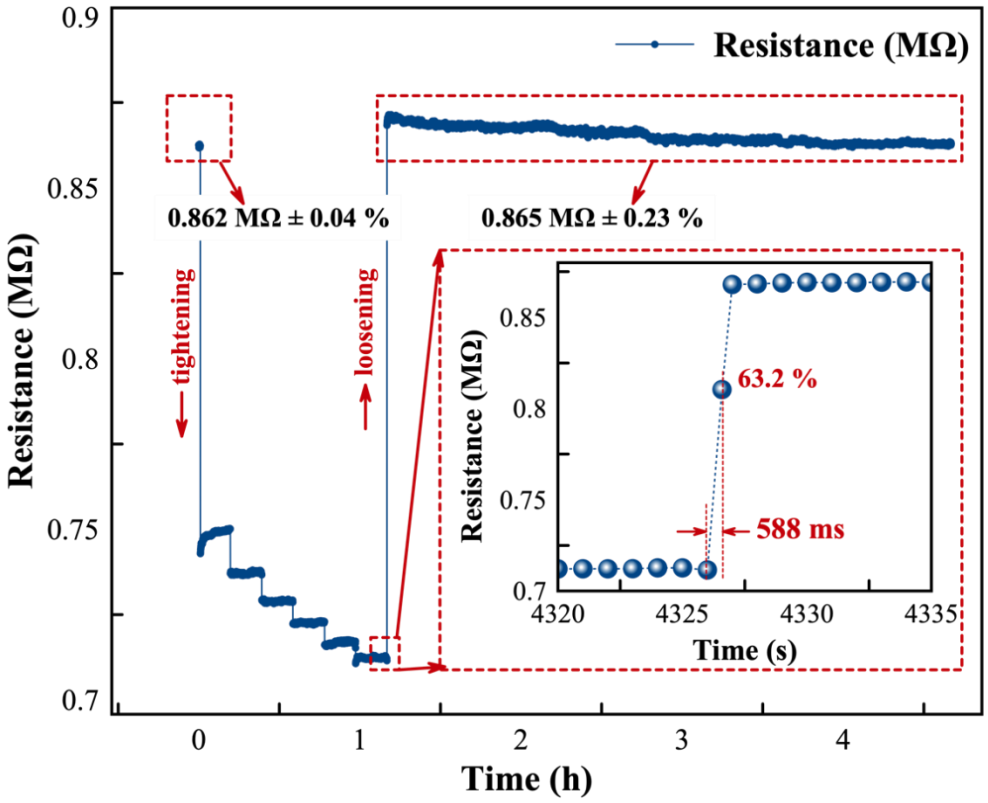

Figure 6: Initial and final resistance profiles of the sensor following the tightening and subsequent loosening of the screw. The inset figure provides further insight into the sensor's reaction time during loosening. Remarkably, the sensor demonstrates an exceptional ability to recover rapidly to its initial position, indicating a swift response characteristic.

We also studied the response time of the sensor (**Fig. 6** inset). When the bolt starts to loosen, the pressure-sensitive layer reacts with a fast response of approximately 588 ms. The rapid reaction of MWCNTs/epoxy nanocomposites is directly linked to the fast re-organization of the MWCNTs network within the epoxy polymer matrix [40,41]. On the other hand, sensor linearity is a crucial parameter because it indicates the consistency of the response of a sensor across its specified measurement range. Depending on the type of application, the non-linear response could be a significant disadvantage for the practical application of the sensor since non-linear responses require complex linearization methods,

curve-fitting, and calibration [40–42]. The proposed sensor has quite a linear piezoresistivity response under applied tightening torque with a linearity factor of 0.96 (Fig. S4), which confirms again that the proposed sensor can be easily used as a pressure sensor in the monitoring of the loosening of the screws in big machines in the industrial plants.

3. Conclusion

BoltWISE is a pressure-sensitive intelligent washer for monitoring the loosening/tightening torques of the bolted joints. BoltWISE can be produced relatively low cost using the stencil printing technique with the materials for prototypes costing less than $1 in our lab. We expect this number to decrease substantially when the production is scaled up industrially. BoltWISE exhibited superior piezoresistive performance compared to existing solutions in terms of sensitivity, hysteresis, response time and linearity. BoltWISE reported in this work, however, has at least four limitations:

(i) We used FR4 as a substrate because of its strong adhesion to the pressure-sensitive layer. FR4, however, tends to fracture under high loads, which, as a result, can cause sensor failure. Using alternative materials, such as steel (with an insulating layer), could overcome this issue.

(ii) The sensor is sensitive to temperature and humidity [43,44]. These effects can be compensated by integrating a dummy sensor (not under load) placed close to the active sensor. This approach would allow the resistance change due to environmental factors to be subtracted from the resistance change under load.

(iii) The current sensor design is unsuitable for non-flat surfaces due to the limitations of the FR4 substrate; however, we have previously demonstrated that the

MWCNTs/epoxy composite can also be deposited on a flexible polyamide substrate. [43,45]

(iv) Data transmission and monitoring of the current version of BoltWISE is not wireless, which could limit its practical application. In future versions, using a mobile device, such as a mobile phone, the data generated by the sensors can be easily processed and stored on the cloud with remote access capabilities, essential for structural health monitoring applications.

BoltWISE demonstrates strong potential as a highly scalable smart washer for monitoring loosening torques in bolted joints of large industrial machines. It offers low service costs and improved sensor performance. While we have focused on loosening torques of the bolted joints in this work, this technology is suitable for a wide range of applications, including anterior cruciate ligament (ACL) surgery and dental implants.

4. Experimental Methods

Deposition of nanocomposite layer and final sensor design: Due to its good mechanical properties and strong adhesion with the nanocomposites, a glass-reinforced epoxy substrate (FR4) is used for thin nanocomposite-based sensor layers [46]. After the dispersion preparation, the FR4 substrate is first covered with a mask for electrode deposition to perform the electrical measurements. Here, a certain amount of silver paste is applied on both sides manually and dried for 30 min at room temperature in a clean chamber to ensure good electrical contact between the nanocomposite layer and the silver paste. Then, a second mask with pre-defined patterns of 3 mm × 5 mm in size is applied on the substrate for nanocomposite deposition. Due to the high viscosity of MWCNTs/epoxy nanocomposite, it is highly challenging to obtain a thin layer. We therefore used a stencil printing technique to deposit MWCNTs/epoxy nanocomposite on the FR4 substrate (**Fig. S1**). After the deposition of the nanocomposite layer and removal of the masks, the sample is dried for 3 h at 160 °C in a climate chamber. Finally, to prevent sensor damage during the load and minimize the humidity influences, a thin layer of latex polymer is applied onto the sensor and dried overnight.

Determination of optimum sensor position and measurement setup: MWCNTs/epoxy nanocomposites-based force sensor deposited on FR4 substrate is located between the washer and steel block (**Fig. S3**). Through a choice of a proper washer, the sensor area is covered to make sure that the pressure is being applied to the sensor layer. In this work, we used a screw with the thread diameter of 10 mm (M10) and strength class of 8.8. According to the datasheet (DIN 13-1), the maximum torque that can be applied to the screw is 33.5

Nm. Since we aim to monitor bolt loosening and protect the sensor from damage, we applied a maximum of 10 Nm of torque to the sensor. A highly precise commercial torque wrench (Neutral, Würth Elektronik) is used to monitor the response of the sensor under applied pressure. The screw is tightened from 5 Nm to 10 Nm with the torque step of 1 Nm, and the corresponding resistance values of the sensor are recorded by a custom-made LabVIEW GUI. For the stability test of the sensor under constant torque, the resistance value of the sensor is recorded over 30 min for each torque step.

Microstructural Characterization: SEM images were acquired using a Nova nanoSEM scanning electron microscope in high vacuum and through the lens detector with immersion mode. To monitor surface topology, Keysight Atomic Force Microscopy (AFM) is used. For imaging, conductive Cr/Pt-coated probes with a diameter of 10 nm, a resonant frequency of 75 kHz, and a force of 3 N/m are used.

Computational modelling of bolt-loosening monitoring system: We used the commercial ANSYS Finite Element (FE) code to conduct FEM investigations. The model used in the analysis consists of an M10 screw, DIN 125-A washer (outer diameter 20 mm, inner diameter 10.5 mm), FR4 substrate and toothed steel block. FEM analysis is performed by the Fasteners module in the Simulation Tool of the PTC Creo© program.

Declaration of Competing Interest

The authors declare that they have no known competing financial interests or personal relationships that could have appeared to influence the work reported in this paper.

Acknowledgements

This work was funded by the Ministry of National Education of Turkey, which provided A.S. and B.D. with scholarships. The authors gratefully acknowledge Torsten Jagermann from Solid Surfaces Analysis, Technische Universität Chemnitz, for guiding the authors during the SEM investigation and Carina Gerlach from Chair of Measurement and Sensor Technology, Technische Universität Chemnitz, for providing the authors with bolts and washers.

Data availability

The raw/processed data required to reproduce these findings cannot be shared at this time due to technical or time limitations.

References

1. Geoffrey L. Kulak, J. W. F. J. H. A. S. *Guide to Design Criteria for Bolted and Riveted Joints*. (2001).
2. Izumi, S., Yokoyama, T., Iwasaki, A. & Sakai, S. Three-dimensional finite element analysis of tightening and loosening mechanism of threaded fastener. *Eng Fail Anal* **12**, 604–615 (2005).
3. Caccese, V., Mewer, R. & Vel, S. S. Detection of bolt load loss in hybrid composite/metal bolted connections. *Eng Struct* **26**, 895–906 (2004).
4. Bickford, J. H. *Introduction to the Design and Behavior of Bolted Joints*. (CRC Press, 2007). doi:10.1201/9780849381874.
5. Wang, Y., Wang, A. X., Wang, Y., Chyu, M. K. & Wang, Q. Sensors and Actuators A : Physical Fabrication and characterization of carbon nanotube – polyimide composite based high temperature flexible thin film piezoresistive strain sensor ☪. *Sens Actuators A Phys* **199**, 265–271 (2013).

6. Gray, L. G. S. & Appleman, B. R. EIS electrochemical impedance spectroscopy - A tool to predict remaining coating life? *Journal of Protective Coatings and Linings* **20**, 66–74 (2003).

7. Nikravesh, S. M. Y. & Goudarzi, M. A Review Paper on Looseness Detection Methods in Bolted Structures. *Latin American Journal of Solids and Structures* **14**, 2153–2176 (2017).

8. Yang, J. & Chang, F.-K. Detection of bolt loosening in C–C composite thermal protection panels: I. Diagnostic principle. *Smart Mater Struct* **15**, 581–590 (2006).

9. Qin, X. *et al.* Full life-cycle monitoring and earlier warning for bolt joint loosening using modified vibro-acoustic modulation. *Mech Syst Signal Process* **162**, 108054 (2022).

10. Jhang, K.-Y., Quan, H.-H., Ha, J. & Kim, N.-Y. Estimation of clamping force in high-tension bolts through ultrasonic velocity measurement. *Ultrasonics* **44**, e1339–e1342 (2006).

11. Roy, T. B. , B. S. , P. S. K. , C. A. , T. L. , & B. A. A novel method for vibration-based damage detection in structures using marginal Hilbert spectrum. in *Recent Advances in Structural Engineering, Volume 1: Select Proceedings of SEC* 1161–1172 (2016).

12. Murakami, T. & Morikawa, H. A method to detect bolt loosening using time-frequency analyses. *J Appl Mech* **9**, 1111–1120 (2006).

13. Huo, L., Chen, D., Kong, Q., Li, H. & Song, G. Smart washer—a piezoceramic-based transducer to monitor looseness of bolted connection. *Smart Mater Struct* **26**, 025033 (2017).

14. Huynh, T.-C., Dang, N.-L. & Kim, J.-T. Preload Monitoring in Bolted Connection Using Piezoelectric-Based Smart Interface. *Sensors* **18**, 2766 (2018).

15. Wang, T., Song, G., Liu, S., Li, Y. & Xiao, H. Review of Bolted Connection Monitoring. *Int J Distrib Sens Netw* **9**, 871213 (2013).

16. Zhang, J., Tian, G., Marindra, A., Sunny, A. & Zhao, A. A Review of Passive RFID Tag Antenna-Based Sensors and Systems for Structural Health Monitoring Applications. *Sensors* **17**, 265 (2017).

17. Mekid, S., Bouhraoua, A. & Baroudi, U. Battery-less wireless remote bolt tension monitoring system. *Mech Syst Signal Process* **128**, 572–587 (2019).

18. Yang, X., Gao, Y., Fang, C., Zheng, Y. & Wang, W. Deep learning-based bolt loosening detection for wind turbine towers. *Struct Control Health Monit* **29**, (2022).

19. Zhao, X., Zhang, Y. & Wang, N. Bolt loosening angle detection technology using deep learning. *Struct Control Health Monit* **26**, e2292 (2019).

20. Nguyen, T.-T., Ta, Q.-B., Ho, D.-D., Kim, J.-T. & Huynh, T.-C. A method for automated bolt-loosening monitoring and assessment using impedance technique and deep learning. *Developments in the Built Environment* **14**, 100122 (2023).

21. Kong, X. & Li, J. Image Registration-Based Bolt Loosening Detection of Steel Joints. *Sensors* **18**, 1000 (2018).

22. Jeong, Y. R. *et al.* Highly Stretchable and Sensitive Strain Sensors Using Fragmentized Graphene Foam. *Adv Funct Mater* **25**, 4228–4236 (2015).

23. Wu, J., Cui, X. & Xu, Y. A Novel RFID-Based Sensing Method for Low-Cost Bolt Loosening Monitoring. *Sensors* **16**, 168 (2016).

24. Martinez, J., Sisman, A., Onen, O., Velasquez, D. & Guldiken, R. A Synthetic Phased Array Surface Acoustic Wave Sensor for Quantifying Bolt Tension. *Sensors* **12**, 12265–12278 (2012).

25. Sun, Y. J., Zhang, Y. H. & Yuan, S. F. Screw Loosening Monitoring in UAV Wing Box Based on Phased Array Theory. *Applied Mechanics and Materials* **303–306**, 533–537 (2013).

26. Qian, Y. *et al.* Quantitative Analysis of Bolt Loosening Angle Based on Deep Learning. *Buildings* **14**, 163 (2024).

27. Sun, Y., Li, M., Dong, R., Chen, W. & Jiang, D. Vision-Based Detection of Bolt Loosening Using YOLOv5. *Sensors* **22**, 5184 (2022).

28. Tanabi, H. & Erdal, M. Effect of CNTs dispersion on electrical, mechanical and strain sensing properties of CNT/epoxy nanocomposites. *Results Phys* **12**, 486–503 (2019).

29. Rao, R. K., Gautham, S. & Sasmal, S. A Comprehensive Review on Carbon Nanotubes Based Smart Nanocomposites Sensors for Various Novel Sensing Applications. *Polymer Reviews* 1–64 (2024) doi:10.1080/15583724.2024.2308889.

30. Park, M., Kim, H. & Youngblood, J. P. Strain-dependent electrical resistance of multi-walled carbon nanotube/polymer composite films. *Nanotechnology* **19**, 055705 (2008).

31. Wichmann, M. H. G., Buschhorn, S. T., Gehrmann, J. & Schulte, K. Piezoresistive response of epoxy composites with carbon nanoparticles under tensile load. *Phys Rev B* **80**, 245437 (2009).

32. Pham, G. T., Park, Y.-B., Liang, Z., Zhang, C. & Wang, B. Processing and modeling of conductive thermoplastic/carbon nanotube films for strain sensing. *Compos B Eng* **39**, 209–216 (2008).

33. Li, C., Thostenson, E. T. & Chou, T.-W. Dominant role of tunneling resistance in the electrical conductivity of carbon nanotube–based composites. *Appl Phys Lett* **91**, (2007).

34. Yu, Y., Song, G. & Sun, L. Determinant role of tunneling resistance in electrical conductivity of polymer composites reinforced by well dispersed carbon nanotubes. *J Appl Phys* **108**, (2010).

35. Simmons, J. G. Electric Tunnel Effect between Dissimilar Electrodes Separated by a Thin Insulating Film. *J Appl Phys* **34**, 2581–2590 (1963).

36. Simmons, J. G. Generalized Formula for the Electric Tunnel Effect between Similar Electrodes Separated by a Thin Insulating Film. *J Appl Phys* **34**, 1793–1803 (1963).

37. Rahman, R. & Servati, P. Effects of inter-tube distance and alignment on tunnelling resistance and strain sensitivity of nanotube/polymer composite films. *Nanotechnology* **23**, 055703 (2012).

38. Amjadi, M., Yoon, Y. J. & Park, I. Ultra-stretchable and skin-mountable strain sensors using carbon nanotubes–Ecoflex nanocomposites. *Nanotechnology* **26**, 375501 (2015).

39. Deng, H. *et al.* Towards tunable resistivity–strain behavior through construction of oriented and selectively distributed conductive networks in conductive polymer composites. *J. Mater. Chem. A* **2**, 10048–10058 (2014).

40. Amjadi, M., Kyung, K., Park, I. & Sitti, M. Stretchable, Skin-Mountable, and Wearable Strain Sensors and Their Potential Applications: A Review. *Adv Funct Mater* **26**, 1678–1698 (2016).

41. Gong, S. *et al.* Highly Stretchy Black Gold E-Skin Nanopatches as Highly Sensitive Wearable Biomedical Sensors. *Adv Electron Mater* **1**, (2015).

42. Medrano-Marques, N. J. & Martin-del-Brio, B. Sensor linearization with neural networks. *IEEE Transactions on Industrial Electronics* **48**, 1288–1290 (2001).

43. Sanli, A. Investigation of temperature effect on the electrical properties of MWCNTs/epoxy nanocomposites by electrochemical impedance spectroscopy. *Advanced Composite Materials* **29**, 31–41 (2020).

44. Sanli, A., Benchirouf, A., Müller, C. & Kanoun, O. Study of the humidity effect on the electrical impedance of MWCNT epoxy nanocomposites. in *Impedance Spectroscopy* 25–32 (De Gruyter, 2018). doi:10.1515/9783110558920-002.

45. Sanli, A., Müller, C., Kanoun, O., Elibol, C. & Wagner, M. F.-X. Piezoresistive characterization of multi-walled carbon nanotube-epoxy based flexible strain sensitive films by impedance spectroscopy. *Compos Sci Technol* **122**, 18–26 (2016).

46. Haugan. E, D. P. *Characterization of the Material Properties of Two FR4 Printed Circuit Board Laminates*. (2014).